

Onsager-Machlup action-based path sampling and its combination with replica exchange for diffusive and multiple pathways

Hiroshi Fujisaki,^{1,2,*} Motoyuki Shiga,^{3,†} and Akinori Kidera^{2,4,‡}

¹ *Department of Physics, Nippon Medical School,*

2-297-2 Kosugi-cho, Nakahara, Kawasaki 211-0063, Japan

² *Molecular Scale Team, Integrated Simulation of Living Matter Group,*

Computational Science Research Program,

RIKEN, 2-1 Hirosawa, Wako 351-0198, Japan

³ *Center for Computational Science and E-Systems,*

Japan Atomic Energy Agency (JAEA),

Higashi-Ueno 6-9-3, Taito-ku, Tokyo 110-0015, Japan

⁴ *Department of Supramolecular Biology,*

Graduate School of Nanobioscience,

Yokohama City University, 1-7-29 Suehiro-cho,

Tsurumi, Yokohama 230-0045, Japan

(Dated: October 26, 2018)

Abstract

For sampling multiple pathways in a rugged energy landscape, we propose a novel action-based path sampling method using the Onsager-Machlup action functional. Inspired by the Fourier-path integral simulation of a quantum mechanical system, a path in Cartesian space is transformed into that in Fourier space, and an overdamped Langevin equation is derived for the Fourier components to achieve a canonical ensemble of the path at a finite temperature. To avoid “path trapping” around an initially guessed path, the path sampling method is further combined with a powerful sampling technique, the replica exchange method. The principle and algorithm of our method is numerically demonstrated for a model two-dimensional system with a bifurcated potential landscape. The results are compared with those of conventional transition path sampling and the equilibrium theory, and the error due to path discretization is also discussed.

*Electronic address: fujisaki@nms.ac.jp

†Electronic address: shiga.motoyuki@jaea.go.jp

‡Electronic address: kidera@tsurumi.yokohama-cu.ac.jp

I. INTRODUCTION

To understand the functions of biomolecules (chemical reactions, conformational change, ligand-binding, protein-protein association etc.), determining reaction paths is an essential step [1]. However, conventional molecular dynamics (MD) simulations often fail to find appropriate reaction paths even with huge computational resources [2]. This is because such reactions cannot be simulated within computationally feasible times, and the sampling efficiency of the reaction can be low especially for large systems. Handling such a rare event is a common issue not only for biomolecular systems such as proteins but also for many physical or chemical systems.

So far, many methodologies have been devised for path search or path sampling in biomolecular systems [1]. The most primitive but powerful method may be umbrella sampling after defining certain reaction coordinates such as the radius of gyration or the number of native contacts [3, 4]. Alternatively, metadynamics has been used to compute free energy surfaces with several reaction coordinates [5]. However, all these methods only work for molecular processes characterized by limited numbers of reaction coordinates that are known *a priori*, and one often fails to describe complex and highly multi-dimensional processes in biomolecular systems. As the computational effort grows exponentially with the number of reaction coordinates (dimensions) increases, it is hopeless to work on the full detail of a high-dimensional free energy landscape. Steered or targeted molecular dynamics is another powerful and well-established path search method [6, 7]. In combination with the Jarzynski equality [8–10], a free energy difference can be calculated by steered MD. However, since the reaction path obtained only follows a predefined direction, it may sometimes result in producing paths with unphysically large deformations of molecules.

More direct approaches to deal with complex multi-dimensional reactions are based on minimization of a physically defined *action functional* associated with a reaction path. Elber and Karplus [11] proposed an innovative approach to use a line integral along a path with some constraints, in search of a minimum energy path such as the intrinsic reaction path [12–14]. This method was successfully applied to peptides [15] and water systems [16]. Other related methods searching for a minimum energy path include the nudged elastic band method [17, 18], the conjugate peak refinement method [19, 20], and the zero-temperature string method [21]. These methods can be used to locate transition state geometries (saddle

points of the potential energy surface, at which barrier crossing can occur with a minimum amount of activation energy), but they do not contain any dynamical information by themselves, since the transition state geometry is merely a static feature of the potential energy landscape. Some kinetic information is retrieved with the use of the discrete path sampling method [22] under the assumptions of transition state theory [23], but the effect of thermal fluctuations, which should be particularly important for biomolecular systems, is not completely captured by these approaches. To include dynamical and thermal effects, transition path sampling (TPS) has been proposed and developed by Chandler and coworkers [24, 25]. The basic idea of TPS is that a system is described by an ensemble of paths instead of a single path. (For a similar and heuristic approach, see [26].) When an overdamped Langevin equation is assumed to describe the dynamics, the weight for a path can be written as

$$P[x(t)] \propto e^{-S[x(t)]/2D} \quad (1)$$

where

$$S[x(t)] = \frac{\Delta U}{\zeta} + \frac{1}{2} \int_0^t ds \left[\dot{x}^2 + \left(\frac{1}{\zeta} \frac{dU}{dx} \right)^2 - \frac{2D}{\zeta} \frac{d^2U}{dx^2} \right] \quad (2)$$

is called the Onsager-Machlup (OM) action “functional” [27, 28] (for its derivation and pedagogic discussions, see, for example, [29]) because it contains all the information of the whole history of a path $x(t)$. Here, $\Delta U = U(x_{\text{fin}}) - U(x_{\text{ini}})$ is the potential energy difference between an initial state with $x_{\text{ini}} = x(0)$ and a final state with $x_{\text{fin}} = x(t)$, D is the diffusion constant, which is related to a friction constant ζ and the absolute temperature T by Einstein’s relation $D = k_B T / \zeta$ (k_B is the Boltzmann constant). TPS intends to sample many paths according to the statistical weight above. Combining conventional MD simulations and Monte Carlo (MC) moves, shooting and shifting [24], TPS has been successfully used for *rare* and *fast* chemical reactions.

However, in biomolecular reactions, such as folding or conformational changes, the process is often not only *rare* but also *slow* and *diffusive*. Protein folding can occur at least more than microsecond timescales, which is still beyond the ability of current “brute-force” MD simulations using “standard” computers and algorithms. This is also the case for conformational change of large protein systems with several domains, which is relevant to the understanding of the functions of proteins [1]. Therefore, alternative approaches to sample path ensembles should be established, and novel hardware strategy [2] and novel theoretical

algorithms including transition interface sampling [30], milestoning [31], and Markov state models [32] have been developed in the last decade.

In this paper, we pursue another approach by discretizing the OM action

$$S = \frac{\Delta U}{\zeta} + \sum_{i=1}^{N-1} \left[\frac{\kappa}{2} (x_{i+1} - x_i)^2 + W(x_i) \right] \quad (3)$$

where $\kappa = 1/\Delta t$, $x_1 = x_{\text{ini}}$, $x_N = x_{\text{fin}}$ and

$$W(x) \equiv \frac{1}{2\kappa} \left[\left(\frac{1}{\zeta} \frac{dU}{dx} \right)^2 - \frac{2D}{\zeta} \frac{d^2U}{dx^2} \right]. \quad (4)$$

The statistical weight is $P(x_1, x_2, \dots, x_N) \propto e^{-S/2D}$, and the path search problem is therefore mapped onto the statistical mechanics of a polymer under the effective potential function $W(x)$ [28]. (This isomorphology is similar to that between a quantum particle and a ring polymer [33].) This strategy was proposed in the original TPS paper [34] but has not been completely worked out. The previous studies using this type of action-based method have mostly focused on a *single* most probable path during conformational changes of biomolecules [35–38]. Here, we try to complete the previous studies and provide a path ensemble at finite temperatures using the action-based method, which should be relevant for slow and diffusive biomolecular reactions.

To generate a path ensemble, we need to assume an initial path, from which the path sampling simulation starts. If there is a barrier in path space, however, the generated path cannot move to the most probable path because “path trapping” occurs in the basin around the initial path (as in the case of “configuration trapping” for the folding problem of proteins). Even worse, for complex systems with rugged energy surfaces, the path to be calculated may not be unique, and multiple paths can coexist. This is the situation we want to address in this paper. In the previous study using the nudged-elastic band, simulated annealing was employed to avoid this “path trapping” problem [18]. This is a nice strategy to sample multiple *minimum energy paths*, however, a path ensemble *at a finite temperature* cannot be obtained. To generate a canonical ensemble for a path, we propose to introduce one of the generalized ensemble methods, the replica exchange method (REM) [39, 40], *in path space*. The combination of REM with transition path sampling has been already proposed [41–43] for rare and fast chemical reactions, however, our aim is to sample rare, slow, and diffusive processes, and the application of the OM action formalism should be more appropriate.

This paper is organized as follows. In Sec. II, we derive an overdamped Langevin equation for a path such that the path ensemble is generated according to the weight determined by the OM action. In parallel to the technique employed in the path integral simulations of quantum systems, we use Fourier components of a path as “dynamic” variables [44]. We then combine this method with REM to improve the sampling efficiency in path space. In Sec. III, we test the numerical performance of our new method. To this end, a two-dimensional model potential due to Bolhuis [43], involving bifurcated reaction pathways, is numerically examined in detail. The results are finally compared with those of TPS and the equilibrium theory. In Sec. IV, we summarize the paper and discuss the connection between our method and other related ones and future development for biomolecules.

II. THEORY

A. Onsager-Machlup action for multi-dimensional systems

To describe slow and diffusive processes, we start from an overdamped Langevin equation for an M -dimensional system using mass-weighted Cartesian coordinates (x_1, \dots, x_M) :

$$\dot{x}_\alpha = -\frac{1}{\gamma_\alpha} \frac{\partial U}{\partial x_\alpha} + \sqrt{2D_\alpha} \eta_\alpha(t) \quad (5)$$

where γ_α is an intrinsic friction coefficient, $\eta_\alpha(t)$ is a Gaussian-white noise satisfying $\langle \eta_\alpha(t) \eta_{\alpha'}(t') \rangle = \delta_{\alpha\alpha'} \delta(t - t')$, and

$$D_\alpha = \frac{k_B T}{\gamma_\alpha} \quad (6)$$

is imposed by the fluctuation-dissipation theorem. The corresponding Fokker-Planck equation [45] is

$$\frac{\partial P(\{x_{\alpha'}\}, t)}{\partial t} = \sum_\alpha \frac{\partial}{\partial x_\alpha} \left(\frac{1}{\gamma_\alpha} \frac{\partial U}{\partial x_\alpha} P(\{x_{\alpha'}\}, t) \right) + \sum_\alpha D_\alpha \frac{\partial^2}{\partial x_\alpha^2} P(\{x_{\alpha'}\}, t). \quad (7)$$

The path-integral representation of the propagator (Green’s function) is written as [29, 38]

$$P(x_{\text{fin}} | x_{\text{ini}}; t) \propto \int_{x(0)=x_{\text{ini}}}^{x(t)=x_{\text{fin}}} \mathcal{D}x(s) e^{-\mathcal{H}[x(s)]/k_B T}, \quad (8)$$

where \mathcal{H} is the OM action defined by the multidimensional extension of Eq. (2), multiplied by $\gamma_\alpha/2$ and summed over α . Its discretized form is written as

$$\mathcal{H} = \frac{\Delta U}{2} + \sum_{i=1}^{N-1} \left[\sum_{\alpha=1}^M \frac{\omega_\alpha^2}{2} (x_{\alpha, i+1} - x_{\alpha, i})^2 + V_{\text{eff}}(\{x_{\alpha, i}\}) \right], \quad (9)$$

where $\Delta U = U(x_{\text{fin}}) - U(x_{\text{ini}})$ and the effective potential is defined as

$$V_{\text{eff}}(\{x_\alpha\}) \equiv \sum_{\alpha=1}^M \left[\frac{1}{8\omega_\alpha^2} U_{x_\alpha}^2 - \frac{k_B T}{4\omega_\alpha^2} U_{x_\alpha x_\alpha} \right] \quad (10)$$

with

$$\omega_\alpha = \sqrt{\frac{\gamma_\alpha}{2\Delta t}} \quad (11)$$

being an effective frequency determined by the friction and the time interval for the path discretization Δt . (Hereafter U_x, U_{xx} represent the first and second derivatives of U with respect to x .) Note that the path ensemble generated by the above OM ‘‘Hamiltonian’’ is isomorphic to the canonical ensemble of an $M \times (N - 2)$ dimensional (polymer) system.

B. Path sampling in Fourier space

For simplicity, we first consider a one-dimensional system. According to Cho, Doll, and Freeman [44], the Fourier transform of a path connecting x_1 and x_N is defined as

$$x_i = x_i^{(0)} + \sqrt{\frac{2}{N-1}} \sum_{k=2}^{N-1} q_k \sin\left(\frac{\pi(i-1)(k-1)}{N-1}\right) = x_i^{(0)} + \sum_{k=2}^{N-1} q_k u_{ik}, \quad (12)$$

where q_k is the Fourier component of the path x_i , and $x_i^{(0)}$ is a reference path, which may be an initially guessed path. To generate a path ensemble with the weight determined by the OM Hamiltonian \mathcal{H} , Eq. (9), the following overdamped Langevin dynamics can be employed

$$\dot{q}_k = -L_k \frac{\partial}{\partial q_k} (\beta_T \mathcal{H}) + \sqrt{2L_k} \eta_k(t), \quad (13)$$

with

$$\langle \eta_k(t) \eta_l(t') \rangle = \delta_{kl} \delta(t - t'), \quad (14)$$

where L_k is an Onsager coefficient representing friction, and $1/k_B \beta_T$ is the temperature of a thermostat, not necessarily equal to the system temperature T . Using the corresponding Fokker-Planck equation, the stationary point is shown to be the equilibrium state $P_{\text{eq}}(\{q_k\}) \propto \exp(-\beta_T \mathcal{H})$ in (discretized) path space. Note that this Langevin dynamics is different from the original Langevin dynamics, Eq. (5), which was motivated from a physical consideration.

Substituting the particular form of the OM Hamiltonian, Eq. (9), into the overdamped Langevin equation, we have

$$\dot{q}_k = -\beta_T L_k \sum_{i=2}^{N-1} u_{ik} \frac{\partial \mathcal{H}}{\partial x_i} + \sqrt{2L_k} \eta_k(t), \quad (15)$$

$$\frac{\partial \mathcal{H}}{\partial x_i} = -\omega^2(x_{i+1} + x_{i-1} - 2x_i) + \frac{\partial V_{\text{eff}}(x_i)}{\partial x_i}, \quad (16)$$

$$\frac{\partial V_{\text{eff}}(x)}{\partial x} = \frac{1}{4\omega^2} U_x U_{xx} - \frac{k_B T}{4\omega^2} U_{xxx}, \quad (17)$$

where ω is the one-dimensional analog of Eq. (11). Finally we obtain

$$\dot{q}_k = G_k - \Gamma_k q_k - \beta_T L_k \sum_{i=2}^{N-1} u_{ik} \frac{\partial V_{\text{eff}}(x_i)}{\partial x_i} + \sqrt{2L_k} \eta_k(t), \quad (18)$$

where

$$G_k = \omega^2 \beta_T L_k \sum_{i=2}^{N-1} u_{ik} (x_{i+1}^{(0)} + x_{i-1}^{(0)} - 2x_i^{(0)}), \quad (19)$$

$$\Gamma_k = 2\omega^2 \beta_T L_k \left(1 - \cos \frac{\pi(k-1)}{N-1} \right). \quad (20)$$

By taking

$$L_k = \frac{1}{\lambda \Delta t \beta_T \omega^2} \left(1 - \cos \frac{\pi(k-1)}{N-1} \right)^{-1}, \quad (21)$$

the rate becomes constant: $\Gamma_k = \Gamma_0 = 2/(\lambda \Delta t)$ where λ is a dimensionless parameter to adjust a timescale for relaxation. This particular form of the Onsager coefficient was chosen because the time step to solve the above series ($k = 2, 3, \dots, N-1$) of Langevin equations may be determined by a single timescale $1/\Gamma_0$.

The Fourier-path Langevin dynamics for the M -dimensional system becomes

$$\dot{q}_{\alpha,k} = G_{\alpha,k} - \Gamma_0 q_{\alpha,k} - \beta_T L_k \sum_{i=2}^{N-1} u_{ik} \left. \frac{\partial V_{\text{eff}}(\{x_\alpha\})}{\partial x_\alpha} \right|_{x_\alpha=x_{\alpha,i}} + \sqrt{2L_k} \eta_{\alpha,k}(t), \quad (22)$$

where

$$\frac{\partial V_{\text{eff}}(\{x_\alpha\})}{\partial x_\alpha} = \sum_{\beta=1}^M \left[\frac{1}{4\omega_\beta^2} U_{x_\beta} U_{x_\beta x_\alpha} - \frac{k_B T}{4\omega_\beta^2} U_{x_\beta x_\beta x_\alpha} \right], \quad (23)$$

and L_k is chosen as in Eq. (21) with $\omega = \omega_\alpha$. Practically, the hessian and its derivative above are the bottleneck of this computation, hampering its application to large molecular systems. Recently, however, the symmetric OM action, which only uses the force to calculate the OM action, has been devised by Miller and Predescu [46]. Such a ‘‘low cost’’ action can be utilized for the future application of this method to real molecular systems.

C. Replica exchange in path space

In the previous subsection, we have obtained a primitive way to generate a path ensemble by solving the overdamped Langevin equation for Fourier components of a path. However, path sampling efficiency becomes an issue in biomolecular simulations due to the extremely rugged-energy surface. In such a case, the sampled path often gets trapped around the initially assumed path, leading to unphysical results and incorrect predictions on the reaction mechanism. This situation is in parallel with the configuration sampling problem of complex molecules such as peptides or proteins in a rugged-energy landscape.

Generalized ensemble methods such as multi-canonical sampling [47, 48] or replica exchange [39, 40] (parallel tempering) are well-known to solve this problem. We here combine one of these methods, the replica exchange method (REM), with the OM method because of its simplicity for implementation. It is easy to derive the following acceptance probability for exchange of two replicas

$$P_{\text{acc}} = \min(1, \exp\{\Delta\}), \quad (24)$$

$$\Delta = (\beta - \beta')(\mathcal{H} - \mathcal{H}'), \quad (25)$$

where (β, \mathcal{H}) and (β', \mathcal{H}') are the inverse temperature and the OM Hamiltonian for each replica. The difference with the conventional REM [39, 40] is that each replica is associated with a path (see Fig. 1), and that Eq. (9) is employed for the effective Hamiltonian \mathcal{H} . As usually done, we prepare several replicas for a path and, during the Langevin dynamics in our case, exchange two “neighboring” paths at the same time with the above probability [40]. If the number of replicas and the exchange rate between replicas are both sufficiently large to sample the whole “path” space, an appropriate path ensemble with temperature T should be obtained by collecting path data indexed by the same T .

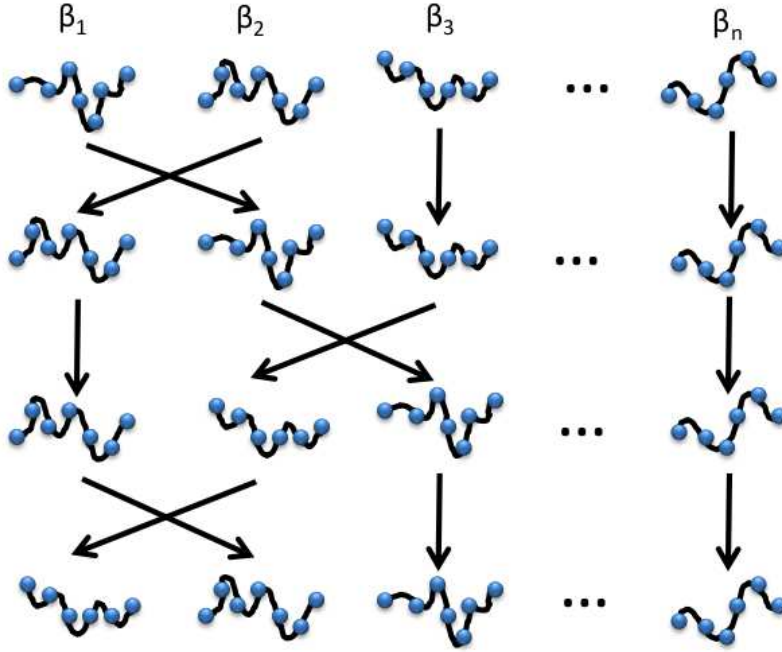


FIG. 1: Schematic drawing of the proposed replica-exchange method for path sampling using the Onsager-Machlup action. Each column represents the OM dynamics of a single path. Different path replicas with different inverse temperatures β_i ($i = 1, 2, \dots, n$) are exchanged according to the Metropolis criterion, Eqs. (24) and (25).

III. RESULTS

A. Model and methods

We test our method by using Bolhuis' two-dimensional potential [43]

$$\begin{aligned}
 U(x, y) = & -3e^{-0.25(x-4)^2-y^2} - 3e^{-0.25(x+4)^2-y^2} \\
 & + \frac{32}{1800}(0.0625x^4 + y^4) + 5e^{-0.0081x^4-4y^2} \\
 & + 2e^{-1.5(x-b)^2-(y-1)^2} + 2ae^{-1.5(x+b)^2-(y+1)^2}.
 \end{aligned} \tag{26}$$

This potential has two minima at $(\pm 4.3, 0.0)$ which are interconnected by two reaction pathways via two saddle points $(0.0, \pm 2.3)$. These pathways are separated by a large energy barrier centered at $(0.0, 0.0)$. The parameters are taken as $a = 1$ and $b = 0$, resulting in a symmetric shape of the potential (see Fig. 2). This potential was chosen because it is a minimal model with multiple pathways, representing the local character of the rugged energy landscape of biomolecules. Our aim is to sample an ensemble of paths connecting

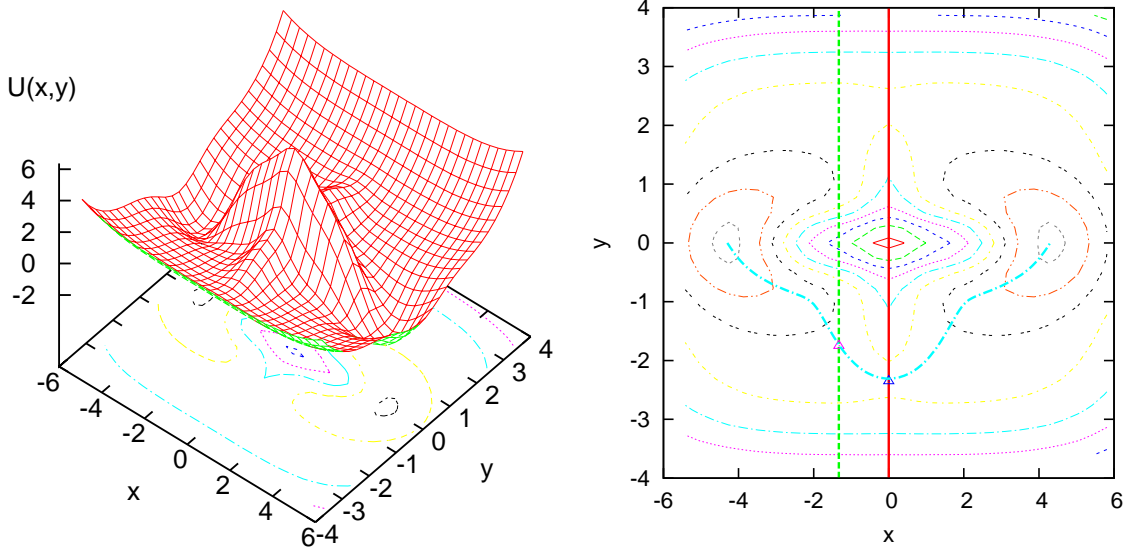


FIG. 2: Left: Bolhuis’ potential defined by Eq. (26) with $a = 1$ and $b = 0$ (symmetric case). There are two stable regions (basins) around $(x, y) = (\pm 4.3, 0)$ and a large barrier separating two pathways connecting the two basins. Right: Contour plot of the Bolhuis potential. The red and green vertical lines represent the exit positions used later in the analysis. The blue curve connecting two minima represents a minimum energy path and the intersections with the red and green lines are denoted as triangles.

two minima.

We need to determine the parameters for the overdamped Langevin equation, Eq. (5). We first take $\gamma_\alpha = 1$, i.e., the characteristic timescale of this Langevin dynamics is unity. From the Einstein relation, Eq. (6), the diffusion constant is equal to the thermal energy, $k_B T$. Here we set $k_B T = 1.25$, since this is an interesting case where barrier crossing can easily occur in the x direction, but not in the y direction.

Next we describe how to discretize a path in the Bolhuis potential. The discretization of a path can be characterized by the time interval Δt and the number of the discretized path (the number of “beads”) N , i.e., the total time of the path is $t_{\text{tot}} = N\Delta t$. To estimate the reasonable value for t_{tot} , we consider free diffusion between the two minima with length L , where the diffusion timescale is $t_{\text{diff}} = L^2/2D$. In our case, $L \simeq 2 \times 4.3 = 8.6$ and $D = 1.25$, and thus $t_{\text{diff}} \simeq 30$. However, if the potential surface is concave in the transition state region, the motion can be quicker than free diffusion, and the actual time for barrier crossing can

be shorter than this estimate. In this paper, we chose $t_{\text{tot}} = 12$. The next question is how to choose Δt or N while $N\Delta t = 12$. After several trial and error, we found that $\Delta t = 0.05$ and $N = 240$ are appropriate for this Bolhuis potential.

We further need to determine the time step for the Fourier-path Langevin dynamics, Eq. (22). We used the simplest Euler scheme to solve this dynamics [49], and found that $\lambda = 10^5$ and $\Delta t_F = 0.5$ are reasonable. Note that the Langevin dynamics for a path is carried out just for sampling and the timescale determined by these parameters have no physical meaning. For comparison, we also numerically solve the original overdamped Langevin equation, Eq. (5), with the same Euler scheme. We have confirmed that $\Delta t_L = 0.003$ is sufficient to recover the potential function through the formula $U(x, y) = -k_B T \log P(x, y) + C$, where $P(x, y)$ is the distribution function calculated by the Langevin trajectory and C is a constant.

Finally we describe how to choose the parameters for REM. The most important prerequisite for REM is that the distribution of \mathcal{H} should have sufficient overlap between neighboring replicas [39, 40], which is written as

$$|\langle \mathcal{H} \rangle_{i+1} - \langle \mathcal{H} \rangle_i| < \langle \Delta \mathcal{H} \rangle_{i+1} + \langle \Delta \mathcal{H} \rangle_i. \quad (27)$$

A rough estimate may be obtained from an independent particle approximation and equipartition principle. For the spring contribution in Eq. (9), the number of particles is approximately $N \times M$, and the thermal energy $k_B T/2$ is given to each degree of freedom, the partial average value of the Hamiltonian \mathcal{H} is therefore $NMk_B T/2$. Actually there is a contribution from the effective potential term V_{eff} , which might be also approximated as an N -tuple connected harmonic spring, then the average of the total Hamiltonian may be $\langle \mathcal{H} \rangle = NMk_B T$. Assuming that they are all uncorrelated Gaussian random numbers, the fluctuations of the Hamiltonian becomes $\langle \Delta \mathcal{H} \rangle = \sqrt{2NM}k_B T$. Defining $f = T_{i+1}/T_i > 1$, the criterion for the neighboring distributions to overlap is written as

$$NM(f - 1) < \sqrt{2NM}(f + 1), \quad (28)$$

and we find

$$1 < f < 1 + \frac{2}{\sqrt{NM/2} - 1}. \quad (29)$$

In our case of the Bolhuis potential, $NM \simeq 480$, the right-hand side thus becomes 1.14. In this paper, we prepare eight replicas by taking $f = 1.14$, hence the corresponding temperatures are $k_B T = 3.60, 3.10, 2.66, 2.29, 1.97, 1.69, 1.46, 1.25$. We have checked that the eight

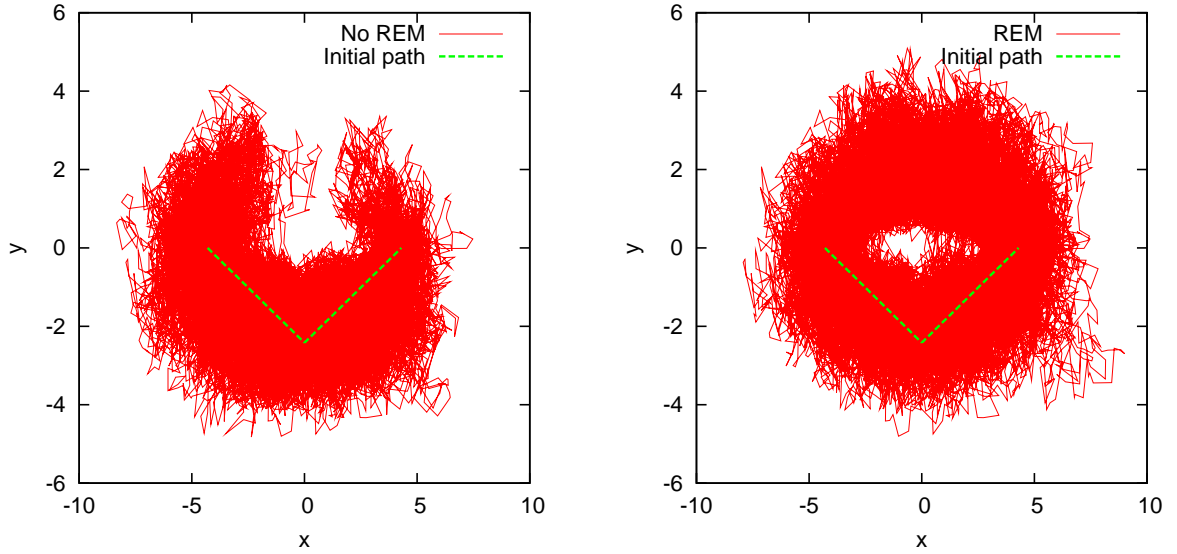


FIG. 3: Path ensemble generated by the Fourier-path dynamics without REM (left) and with REM (right). The diffusion constant or temperature is $D = k_B T = 1.25$. 200 paths are superimposed for each panel with the interval of $30 \times \Delta t_F$. The initial guess is also drawn as a green line.

replicas are mixed up well and the equilibrium path distributions are sampled appropriately at the respective temperatures.

B. Numerical results

In Fig. 3, we show the path ensembles generated by the Fourier-path dynamics with (right) or without (left) the use of REM. An initially guessed path (green line in Fig. 3) was shifted from a linearly interpolated path to avoid the energy being too high. Starting from the initial path, the generated path gradually spreads out in path space. However, in this “timescale” ($200 \times 30 \times \Delta t_F$), the path sampling without REM is not sufficient because the distribution turns out not to be symmetric (see the left of Fig. 3). This indicates that the simple Fourier-path dynamics does not converge fast enough when there are multiple pathways: this is the situation of “path trapping” that we may encounter in path sampling simulations of biomolecules. For such a case, REM should be employed to improve the sampling in path space. As shown in the right of Fig. 3, the Fourier-path dynamics with REM can explore larger path space, resulting in a more symmetrical distribution as expected.

From the path ensemble thus generated, we can obtain both nonequilibrium (such as

kinetic rates) and equilibrium properties (such as free energy profiles). Since we want to examine the nonequilibrium properties of the path ensemble, we employ an *exit distribution* [50] as a measure of such nonequilibrium properties. Note that the exit distribution is conceptually different from a free energy surface which is defined for equilibrium systems. For our model system, the exit distribution is defined as a histogram of accumulated y when a trajectory first hits a cross section $x = x_{\text{exit}}$. In Fig. 4, we show the numerical result of the exit distributions for two exit positions: (a) one is on the transition state (TS): $x_{\text{exit}} = 0$, corresponding to the red line in Fig. 2, and (b) the other is apart from the TS: $x_{\text{exit}} = -1.33$, corresponding to the green line in Fig. 2. Because it is located on TS, case (a) is expected to show stronger nonequilibrium behavior than case (b). To check the correctness of our result, we also show the exit distributions calculated by transition path sampling (TPS) using the algorithm due to Crooks and Chandler [50]. For the TPS calculations, the total time was $t_{\text{tot}} = 12$ as we used in the Fourier-path dynamics calculation, and a small cutoff distance (0.05) was introduced to define the reactant and product states around two minima. We see that two exit distributions calculated by the two methods (at the different exit positions) agree well within the statistical error. This result indicates that our method using the OM action with REM can be alternative to TPS. From computational points of view, for this type of “small” system, TPS works best because it can easily sample the whole path space using the Crooks-Chandler algorithm. The algorithm due to Eastman, Gronbeck-Jensen, and Doniach [37] is almost comparable to ours because both methods use the same information of the system such as the derivative of a hessian matrix. Note, however, that our intention is to present an efficient path sampling algorithm for large systems. This approach of path sampling is considered to be more feasible for slow processes in large systems.

Next, the exit distributions are compared to the equilibrium probability function (PDF) at the exit points, which is calculated as

$$P_{\text{eq}}(y) \propto \exp\{-\beta U(x_{\text{exit}}, y)\} \quad (30)$$

after normalization along the y direction. It is interesting to see that although the PDF is conceptually different from the exit distribution, they look similar to each other at $x_{\text{exit}} = -1.33$ (case (b), see the right of Fig. 4). On the other hand, the exit distribution is quite different from the PDF at $x_{\text{exit}} = 0.0$ (case (a), see the left of Fig. 4), which should be attributed to nonequilibrium effects. We have also computed the exit distributions using

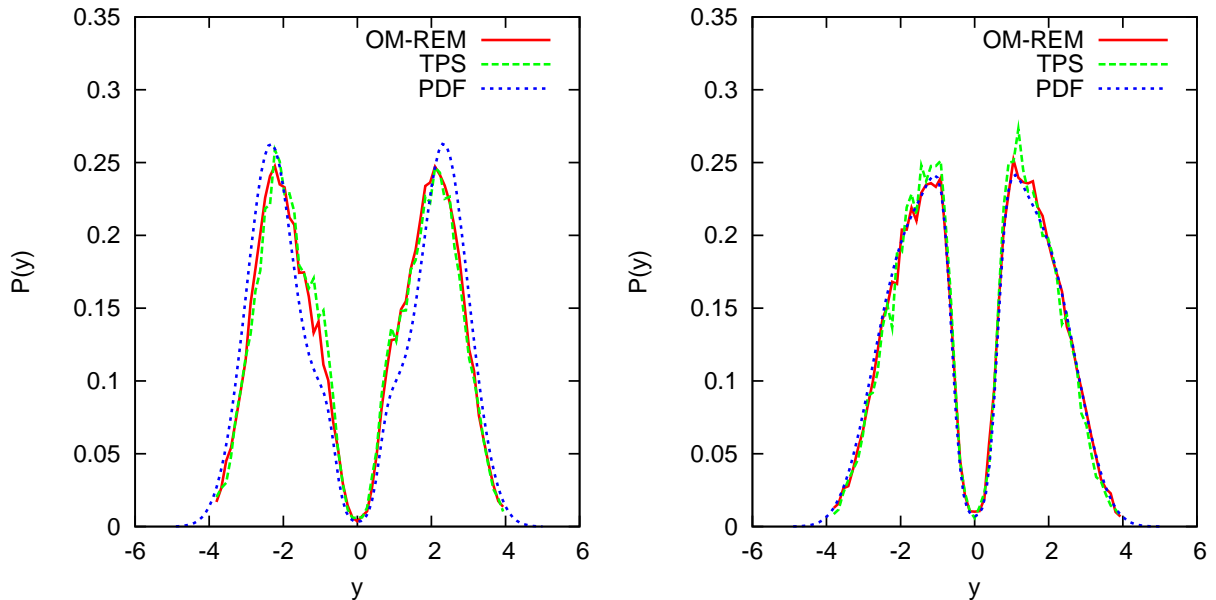


FIG. 4: Exit distributions on the transition state ($x_{\text{exit}} = 0$, left, corresponding to the red line on the right panel of Fig. 2) and apart from the TS ($x_{\text{exit}} = -1.33$, right, corresponding to the green line on the right panel of Fig. 2) calculated by the OM method with REM (red) and TPS (green) with $D = k_B T = 1.25$. The equilibrium probability distribution function (PDF) is also shown (blue).

direct Brownian dynamics starting from one minimum (data not shown). Interestingly, the result also gives a similar exit distribution for case (a) but not for case (b). This indicates that the exit distribution does depend on the final state as well as the initial state, and for case (b) such an effect can be significant. As such, our method or TPS should be carefully compared with direct Brownian dynamics.

The calculations done have been so far successful, and we now discuss practical aspects of the path sampling simulations. In our approach, one of the important parameters that affect the computational effort is the length for path discretization Δt . It is thus useful to mention how and why the calculation fails when we take larger Δt . In the left of Fig. 5, we show the result of the exit distribution with $\Delta t = 0.1$ and $N = 120$ for case (a) while fixing the total time $t_{\text{tot}} = 12$ (the original setting was $\Delta t = 0.05$ and $N = 240$). Compared with the left of Fig. 4, one can see that spurious peaks appear around $x = \pm 1.0$.

To understand these peak structures, we carefully examine the effective potential, Eq. (10). This potential can be decomposed into two parts: one is the zero-temperature

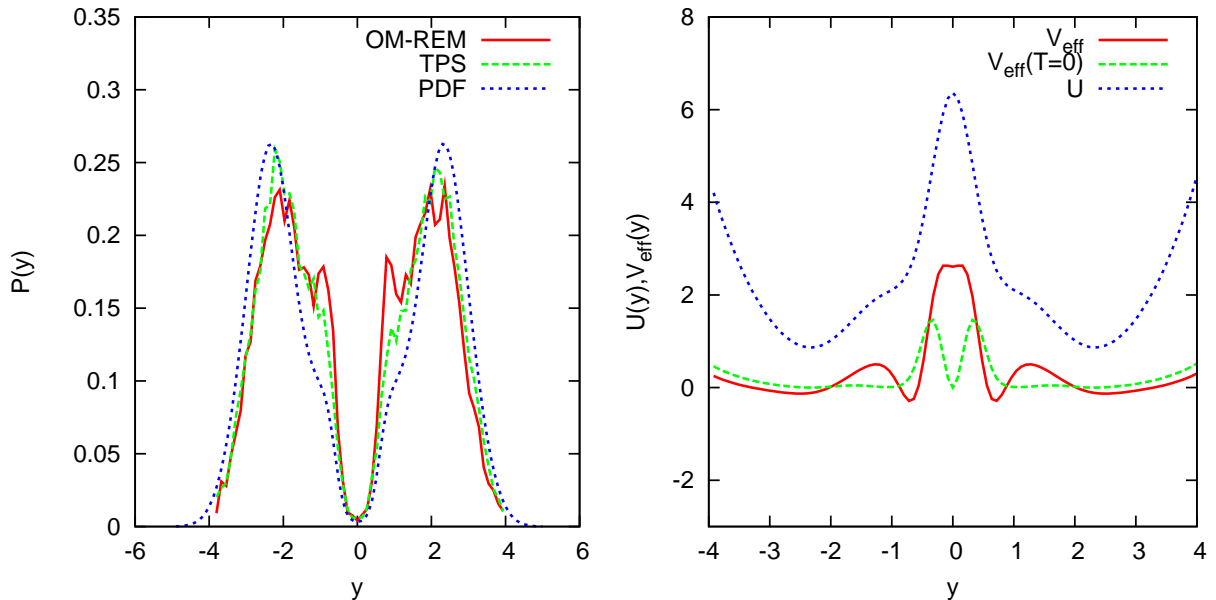


FIG. 5: Left: Exit distributions calculated by our method and TPS at the exit position $x_{\text{exit}} = 0$ with $k_B T = 1.25$. For the OM calculation, $\Delta t = 0.1$ and $N = 120$ were chosen for the path discretization. The probability distribution function at the exit position is also shown as a reference. Right: Cross sections of the effective potential (red) and its zero-temperature component (green) at the exit position $x_{\text{exit}} = 0$ with $k_B T = 1.25$. The cross section of the potential energy function is also shown in blue.

component $V_{\text{eff}}^{(1)}(\{x_\alpha\})$ and the other the finite-temperature component $V_{\text{eff}}^{(2)}(\{x_\alpha\})$, that is,

$$V_{\text{eff}}(\{x_\alpha\}) = V_{\text{eff}}^{(1)}(\{x_\alpha\}) + V_{\text{eff}}^{(2)}(\{x_\alpha\}), \quad (31)$$

$$V_{\text{eff}}^{(1)}(\{x_\alpha\}), = \sum_{\alpha=1}^M \frac{1}{8\omega_\alpha^2} U_{x_\alpha}^2, \quad (32)$$

$$V_{\text{eff}}^{(2)}(\{x_\alpha\}) = -k_B T \sum_{\alpha=1}^M \frac{1}{4\omega_\alpha^2} U_{x_\alpha x_\alpha}. \quad (33)$$

It is easily seen that the finite-temperature component becomes zero when $T = 0$. More importantly, the finite-temperature component prefers a path with positive and large curvatures. This is because an ensemble of trajectories becomes stable in the region where a curvature is large. (If the curvature is negative, the ensemble is unstable and spreading.)

In the right of Fig. 5, we show the cross sections at the exit points for $V_{\text{eff}}^{(1)}$ and V_{eff} . From this figure, we can clearly see that the zero-temperature component does not have a sufficient ability to drag the path around $y \simeq \pm 1.0$. We thus conclude that the peak structures in the exit distribution stem from the finite-temperature component of the effective potential.

Hence we need to be careful when we deal with a path ensemble with large Δt because some spurious features such as the peak structures might appear.

IV. CONCLUDING REMARKS

As a novel approach to sample diffusive paths based on the Onsager-Machlup action, we have proposed Fourier-path Langevin dynamics. To achieve powerful sampling in path space and to avoid the problem of “path trapping” around an initially guessed path, we have also suggested to combine this scheme with a powerful sampling technique, the replica exchange method. Using the two dimensional model potential due to Bolhuis, the validity of our method has been confirmed by the numerical comparison to the conventional transition path sampling. We have also identified an interesting nonequilibrium path ensemble near the transition state of the model system, which is different from an equilibrium distribution.

We are now in a position to discuss the relation of our method with other path search or path sampling methods. First, our main concern is the effects of temperature on a path, so the path search methods at a finite temperature such as MaxFlux methods [51, 52], the temperature-dependent reaction coordinate [53], or finite-temperature string methods [54, 55] have strong similarity with our method. The difference is that a path generated by our method still holds nonequilibrium properties of the path and there is no assumption such as the existence of local equilibrium. It is interesting and important to investigate how the path ensembles calculated by different methods are actually different.

In this paper, for simplicity, we assumed overdamped Langevin dynamics, but this restriction can be easily relaxed. We can employ a modified action derived from the underdamped Langevin dynamics instead of the OM action [56]. This strategy was successfully used for dynamic reweighting of a trajectory for a model system [57]. When we apply this method to real molecular systems, we need to judge which Langevin dynamics (overdamped or underdamped) is more appropriate.

Of course, Eq. (13) is not the only dynamics that can generate a canonical ensemble of a path, e.g., one may use NVT molecular dynamics with N ose-Hoover thermostat techniques [58, 59]. In principle, a much simpler algorithm can be used such as a Monte Carlo (MC) move in path space. That is, we devise a certain MC move $x \rightarrow x'$, and accept or reject the move using the Metropolis criterion [42]. However, we need a clever move when we apply

the MC algorithm to biomolecular systems, otherwise the move is rarely accepted. The reason for this deficiency is the same as why a simple MC move does not work for sampling in biomolecular configuration space, i.e., a MC move without consideration of a molecular configuration causes a high energy state which will be rejected [60]. If we can devise a clever move in path space, it would be a powerful alternative to sample path space. Combining the OM method with the other generalized ensemble methods such as the multi-canonical method [47, 48] or the Tsallis ensemble method [61, 62] is also possible and promising.

We are grateful to Artur Adib for sending us a TPS code, and to Yuji Sugita, Tohru Terada, Ikuo Fukuda, Kei Moritsugu, Mikito Toda, and Hiroshi Teramoto for useful discussions. This research was supported by Research and Development of the Next-Generation Integrated Simulation of Living Matter, a part of the Development and Use of the Next-Generation Supercomputer Project of the Ministry of Education, Culture, Sports, Science and Technology (MEXT).

-
- [1] S. Fuchigami, H. Fujisaki, Y. Matsunaga, and A. Kidera, *Protein Functional Motion: Basic Concepts and Computational Methodologies*, Adv. Chem. Phys. (in press).
 - [2] J.L. Klepeis, K. Lindorff-Larsen, R.O. Dror, and D.E. Shaw, *Curr. Opin. Struc. Biol.* **19**, 120 (2009).
 - [3] G.M. Torrie and J.P. Valleau, *J. Comp. Phys.* **23**, 187 (1977).
 - [4] M. Souaille and B. Roux, *Comp. Phys. Commun.* **135**, 40 (2001).
 - [5] A. Laio and M. Parrinello, *Proc. Nat. Acad. Sci. (USA)* **99**, 12562 (2002).
 - [6] B. Isralewitz, M. Gao, and K. Schulten, *Curr. Opin. Struc. Biol.* **11**, 224 (2001).
 - [7] A. van der Vaart, *Theor. Chem. Acc.* **116**, 183 (2006).
 - [8] C. Jarzynski, *Phys. Rev. Lett.* **78**, 2690 (1997).
 - [9] G.E. Crooks, *J. Stat. Phys.* **90**, 1481 (1998).
 - [10] S. Park and K. Schulten, *J. Chem. Phys.* **120**, 5946 (2004).
 - [11] R. Elber and M. Karplus, *Chem. Phys. Lett.* **139**, 375 (1987).
 - [12] K. Fukui, *Acc. Chem. Res.* **14**, 363 (1981).
 - [13] K. Müller, *Angew. Chem. Int. Ed. Engl.* **19**, 1 (1980).
 - [14] J. Ribas-Arino, M. Shiga, and D. Marx, *Angew. Chem. Int. Ed. Engl.* **48**, 4190 (2009).

- [15] R. Czerminski and R. Elber, *Int. J. Quant. Chem.* **24**, 167 (1990).
- [16] I. Ohmine and H. Tanaka, *Chem. Rev.* **93**, 2545 (1993).
- [17] H. Jónsson, G. Mills, and K.W. Jacobsen, in *Classical and Quantum Dynamics in Condensed Phase Simulations*, edited by B.J. Berne, G. Ciccotti and D.F. Coker, World Scientific (1998).
- [18] D.H. Mathews and D.A. Case, *J. Mol. Biol.* **357**, 1683 (2006).
- [19] S. Fischer and M. Karplus, *Chem. Phys. Lett.* **194**, 252 (1992).
- [20] S. Fischer, B. Windshuegel, D. Horak, K.C. Holmes, and J.C. Smith, *Proc. Nat. Acad. Sci. (USA)* **102**, 6873 (2005).
- [21] W. E, W. Ren, and E. Vanden-Eijnden, *J. Chem. Phys.* **126**, 164103 (2007).
- [22] D.J. Wales, *Mol. Phys.* **100**, 3285 (2002); D.J. Wales, *Energy Landscapes*, Cambridge Univ. Press (2003).
- [23] B.J. Berne, M. Borkovec, and J.E. Straub, *J. Phys. Chem.* **92**, 3711 (1988).
- [24] C. Dellago, P.G. Bolhuis, and P.L. Geissler, *Adv. Chem. Phys.* **123**, 1 (2002).
- [25] C. Dellago and P.G. Bolhuis, *Top. Curr. Chem.* **268**, 291 (2007).
- [26] G. Stock, K. Ghosh, and K.A. Dill, *J. Chem. Phys.* **128**, 194102 (2008).
- [27] L. Onsager and S. Machlup, *Phys. Rev.* **91**, 1505 (1953).
- [28] F.W. Wiegell, *Introduction to Path-Integral Methods in Physics and Polymer Science*, World Scientific, Singapore (1986).
- [29] A.B. Adib, *J. Phys. Chem. B* **112**, 5910 (2008).
- [30] J. Juraszek and P.G. Bolhuis, *Biophys. J.* **95**, 4246 (2008).
- [31] R. Elber, *Biophys. J.* **92**, L85 (2007).
- [32] X.H. Huang, G.R. Bowman, S. Bacallado, and V.S. Pande, *Proc. Nat. Acad. Sci. (USA)* **106**, 19765 (2009).
- [33] D. Chandler and P.G. Wolynes, *J. Chem. Phys.* **74**, 4078 (1981).
- [34] C. Dellago, P.G. Bolhuis, F.S. Csajka, and D. Chandler, *J. Chem. Phys.* **108**, 1964 (1998).
- [35] R. Olender and R. Elber, *J. Chem. Phys.* **105**, 9299 (1996); R. Olender and R. Elber, *J. Mol. Struct. Theochem* **398-399**, 63 (1997); R. Elber, J. Meller and R. Olender, *J. Phys. Chem. B*, **103**, 899 (1999); R. Elber, A. Ghosh, and A. Cardenas, *Acc. Chem. Res.* **35**, 396 (2002).
- [36] D.M. Zuckerman and T.B. Woolf, *J. Chem. Phys.* **111**, 9475 (1999).
- [37] P. Eastman, N. Gronbech-Jensen, and S. Doniach, *J. Chem. Phys.* **114**, 3823 (2001).
- [38] P. Faccioli, M. Sega, F. Pederiva, and H. Orland, *Phys. Rev. Lett.* **97**, 108101 (2006); M. Sega,

- P. Faccioli, F. Pederiva, G. Garberoglio, and H. Orland, *ibid.* **99**, 118102 (2007); E. Autieri, P. Faccioli, M. Sega, F. Pederiva, and H. Orland, *J. Chem. Phys.* **130**, 064106 (2009).
- [39] U.H.E. Hansmann, *Chem. Phys. Lett.* **281**, 140 (1997).
- [40] Y. Sugita and Y. Okamoto, *Chem. Phys. Lett.* **314**, 141 (1999).
- [41] T.J.H. Vlugt and B. Smit, *PhysChemComm* **2**, 1 (2001).
- [42] D. Frenkel and B. Smit, *Understanding Molecular Simulation: From Algorithms to Applications*, 2nd ed., Academic Press (2002).
- [43] P.G. Bolhuis, *J. Chem. Phys.* **129**, 114108 (2008).
- [44] A.E. Cho, J.D. Doll, and D.L. Freeman, *Chem. Phys. Lett.* **229**, 218 (1994).
- [45] H. Risken, *The Fokker-Planck Equation: Methods of Solutions and Applications*, 2nd edition, (Springer, 1996).
- [46] T.F. Miller III and C. Predescu, *J. Chem. Phys.* **126**, 144102 (2007).
- [47] N. Nakajima, H. Nakamura, and A. Kidera, *J. Phys. Chem. B* **101**, 817 (1997).
- [48] T. Terada, Y. Matsuo, and A. Kidera, *J. Chem. Phys.* **118**, 4306 (2003).
- [49] A. Greiner, W. Strittmatter, and J. Honerkamp, *J. Stat. Phys.* **51**, 95 (1988).
- [50] G.E. Crooks and D. Chandler, *Phys. Rev. E* **64**, 026109 (2001).
- [51] S.H. Huo and J.E. Straub, *J. Chem. Phys.* **107**, 5000 (1997).
- [52] R. Crehuet and M.J. Field, *J. Chem. Phys.* **118**, 9563 (2003); A. Jiménez and R. Crehuet, *Theor. Chem. Acc.* **118**, 769 (2007).
- [53] R. Elber and D. Shalloway, *J. Chem. Phys.* **112**, 5539 (2000).
- [54] W. E, W. Ren, and E. Vanden-Eijnden, *J. Phys. Chem. B* **109**, 6688 (2005).
- [55] E. Vanden-Eijnden and M. Venturoli, *J. Chem. Phys.* **130**, 194103 (2009).
- [56] S. Machlup and L. Onsager, *Phys. Rev.* **91**, 1512 (1953).
- [57] J. MacFadyen, J. Wereszczynski, and I. Andricioaei, *J. Chem. Phys.* **128**, 114112 (2008).
- [58] S. Nöse, *J. Chem. Phys.* **81**, 511 (1984); W.G. Hoover, *Phys. Rev. A* **31**, 1695 (1985).
- [59] G.J. Martyna, M.L. Klein, and M. Tuckerman, *J. Chem. Phys.* **97**, 2635 (1992).
- [60] A. Kidera, *Int. J. Quant. Chem.* **75**, 207 (1999); H. Yamashita, S. Endo, H. Wako, and A. Kidera, *Chem. Phys. Lett.* **342**, 382 (2001).
- [61] I. Andricioaei and J.E. Straub, *J. Chem. Phys.* **107**, 9117 (1997).
- [62] J. Kim and J.E. Straub, *J. Chem. Phys.* **130**, 144114 (2009).